Journal of Alloys and Compounds 495 (2010) 520–523

Contents lists available at ScienceDirect

Journal of Alloys and Compounds

journal homepage: www.elsevier.com/locate/jallcom

Superparamagnetism in AFM Cr_2O_3 nanoparticles

D. Tobia*, E.L. Winkler, R.D. Zysler, M. Granada, H.E. Troiani

Centro Atómico Bariloche, CNEA-CONICET, Bustillo 9500, 8400 S.C. de Bariloche, Río Negro, Argentina

ARTICLE INFO

Article history:
Received 4 July 2008
Received in revised form 8 October 2009
Accepted 9 October 2009
Available online 20 October 2009

Keywords:
Nanostructured materials
Chemical synthesis
Electron paramagnetic resonance
Magnetic measurements
TEM

ABSTRACT

In this work we report the size effects on the magnetic properties of AFM Cr_2O_3 nanoparticles. From transmission electron microscopy we determined that the system presents high crystallinity and narrow lognormal size distribution centred at $\langle\phi\rangle = 7.8$ nm with $\sigma = 0.3$. The magnetic properties of the nanoparticles were studied by magnetization and electron paramagnetic resonance (EPR) experiments. By EPR spectroscopy we established that the AFM order temperature, T_N, shifted to ~270 K when the size is reduced (T_N(Bulk) ~ 308 K). From the zero-field-cooling and the field-cooling magnetization curves we determined the blocking temperature $T_B = 28$ K. Below T_B the system presents exchange bias effect. We discuss the results by using recent models in terms of the internal magnetic structures of the nanoparticles.

1. Introduction

Surface and size effects in magnetic particles have been subject of increasing interest in the past few decades. Experimental studies of magnetic granular nanosystems have focused the attention on a better degree of control of size and magnetic anisotropy distribution. Any application of these systems in nanoscience or technology requires complete control and understanding of the thermal effects, which have an important role on the magnetic moment relaxation.

When the size of the particles is reduced to nanometric scale, the surface to volume ratio increases and as a result the surface effects become more and more important, affecting the internal magnetic order and the magnetic phase transitions. In the special case of the antiferromagnetic (AFM) nanoparticles it is commonly observed a significant increase of the magnetic moment due to the spin non-compensation at the surface as the particle size is reduced [1,2]. The size effects also lead to other interesting phenomena, such as superparamagnetism, coercivity loops and exchange bias [3].

In this work we investigate the magnetic properties of fine AFM Cr_2O_3 nanoparticles that exhibit superparamagnetic behaviour at low temperature. We analyse the size effects on the parameters that characterize the AFM nanoparticles system. The Cr_2O_3 crystallizes with the corundum structure in the R(-3)*c* space group with a unique three-fold axis along the (1 1 1) direction. Below the Néel temperature, T_N, the four Cr spins in the unit cell are aligned along the uniaxial (1 1 1) crystal axis [4].

2. Experimental

The Cr_2O_3 nanoparticles were synthesized from $Cr(OH)_3$ by chemical route [5]. We mixed an aqueous solution of $Cr(NO_3)_3{\cdot}9H_2O$ with an aqueous solution of Na(OH), under magnetic agitation at pH ≅ 11.5. We centrifuged and washed the solution several times to eliminate the hydroxide excess and then kept the solution in a reflux system at ~380 K, maintaining the magnetic agitation, for four days. We performed differential thermal analysis and thermogravimetric measurements (DT–TGA) in O_2 atmosphere on the obtained powder in order to determine the temperature where the $Cr(OH)_3$ was fully transformed ($T = 680$ K, see inset in Fig. 1). According to these results we calcined the synthesis product in O_2 atmosphere at 773 K in order to obtain the Cr_2O_3 nanoparticles.

The crystalline structure was investigated by X-ray diffraction (XRD) and the morphological characterization was made by transmission electron microscopy (TEM) in a Philips CM200 UT electron microscope, operating at 200 kV. The magnetic characterization of the samples was done using commercial SQUID magnetometers (Quantum Design) with fields up to 70 kOe and in the 5–330 K temperature range. The electron paramagnetic resonance (EPR) spectra were recorded by a Bruker ESP300 spectrometer at 9.5 GHz, in the 5–300 K temperature range.

3. Results and discussions

The powder X-ray diffraction pattern of the synthesized powder corresponds to the R(-3)*c* Cr_2O_3 phase as it is depicted in Fig. 1. TEM images show nearly round shape nanoparticles with high crystallinity. By high resolution TEM images it can be clearly identified the (0 1 2) planes corresponding to the interplanar distance $d = 3.636$ (5) Å (see Fig. 2) and (1 0 4) corresponding to $d = 2.655$ (1) Å. In the inset of Fig. 2 we show the size distribution histogram which presents a lognormal distribution with mean diameter $\langle\phi\rangle = 7.8$ nm and $\sigma = 0.3$.

We performed magnetization vs. temperature measurements $M(T)$ under zero-field-cooling (ZFC) and field-cooling (FC) conditions, from 5 to 330 K. In Fig. 3 we present the magnetization

* Corresponding author. Tel.: +54 2944 445158; fax: +54 2944 445299.
E-mail address: dina.tobia@cab.cnea.gov.ar (D. Tobia).

0925-8388/$ – see front matter © 2009 Elsevier B.V. All rights reserved.
doi:10.1016/j.jallcom.2009.10.060

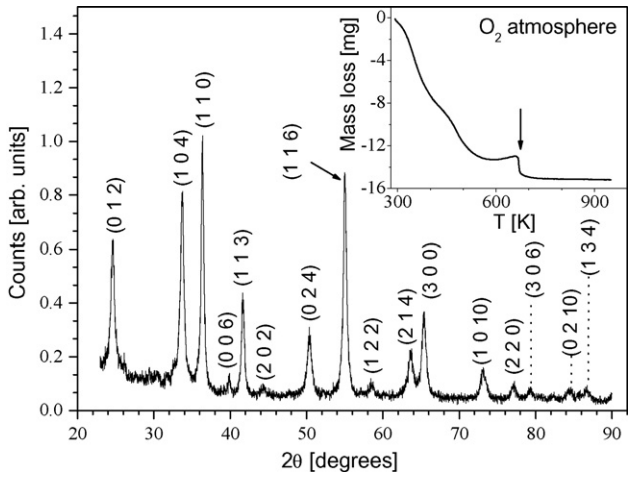

Fig. 1. Indexed X-ray (Cu Kα) diffraction pattern of the Cr_2O_3 nanoparticles. Inset: thermogravimetric (TGA) measurement.

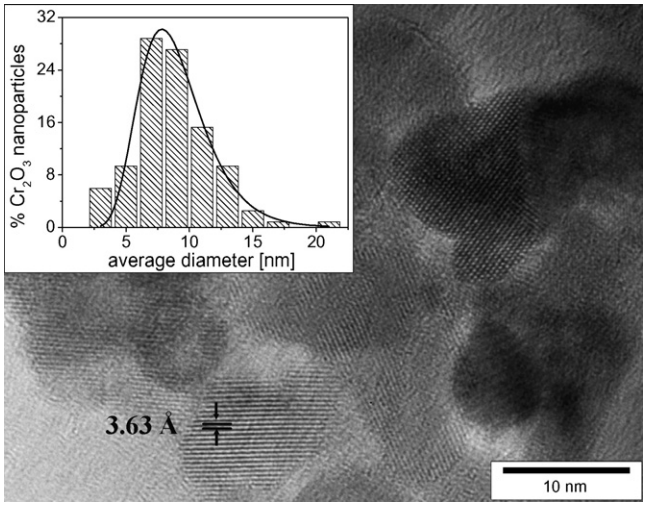

Fig. 2. High resolution TEM image of the sample. Inset: particle size distribution as evaluated from TEM images.

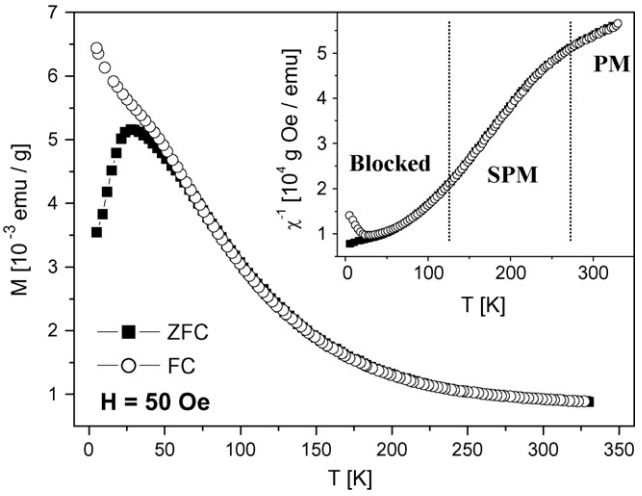

Fig. 3. Temperature dependence of the ZFC (solid symbols) and FC (open symbols) magnetization measured in a field of 50 Oe. Inset: inverse of the susceptibility vs. temperature.

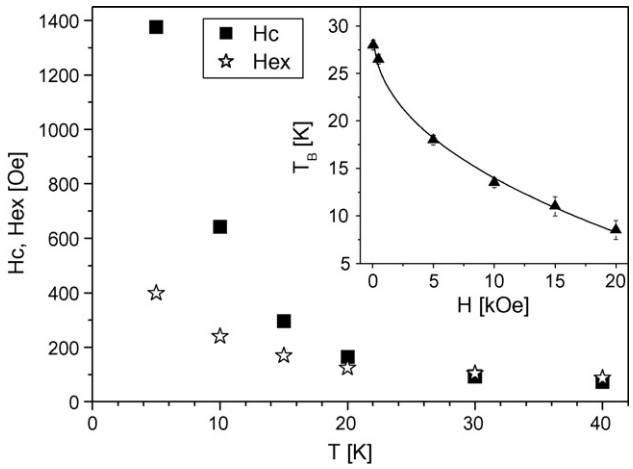

Fig. 4. Coercive field and exchange field temperature dependence. Inset: blocking temperature as a function of the applied magnetic field.

curve measured with an applied field $H = 50$ Oe, where an irreversibility between the M_{ZFC} and the M_{FC} curves is observed at low temperature. M_{ZFC} exhibits a narrow maximum centred at $T_B = 28$ K, characteristic of a change from a superparamagnetic to a blocked behaviour. From the inverse of the susceptibility it can be clearly distinguished three magnetic regimes (see inset of Fig. 3). At high temperature ($T > 280$ K) the system presents Curie–Weiss behaviour, which is in agreement with the paramagnetic (PM) behaviour of the Cr^{3+} ions. At intermediate temperature range, χ^{-1} also presents a lineal dependence with T as it is expected for a superparamagnetic nanoparticles array. Finally, an irreversible behaviour is observed at the low temperature region, which corresponds to the blocked regime. From the comparison between the superparamagnetic and the PM slope we can deduce that $N\mu_{eff}^2 > n\mu_{NP}^2$, where μ_{eff} is the Cr^{3+} effective magnetic moment, N is the number of Cr^{3+} ions per gram, μ_{NP} is the nanoparticle magnetic moment and n is the number of nanoparticles per gram. The μ_{NP} value will be evaluated from the Langevin law followed by the M vs. H curves. At this point it is noteworthy that the PM behaviour observed down to $T \sim 280$ K implies that the magnetic ordering temperature decreases from the bulk value $T_N \sim 308$ K when the size is reduced. This fact will be confirmed below by the EPR experiments.

The maximum of the M_{ZFC} curve shifts to lower temperatures for increasing applied fields and for fields higher than 30 kOe T_B is not longer observed (inset Fig. 4). The field dependence of T_B follows a power law $T_B = T_0\ (1 - (H/H_0)^{\beta})$ (solid line in the inset of Fig. 4), where $T_0 = 30 \pm 1$ K, $H_0 = 42 \pm 5$ kOe and $\beta = 0.44 \pm 0.06$. Note that the obtained β parameter is smaller than the $\beta = 2/3$ theoretically predicted by Dormann et al. [6] for a non-interacting nanoparticles system.

The field dependence of the magnetization exhibits different behaviours at different temperatures. At room temperature the magnetization presents a lineal dependence with the magnetic field in agreement with the PM state of the Cr^{3+} ions. At intermediate temperature $T_B < T < T_N$, the $M(H)$ curves are reversible and show a curvature characteristic of a superparamagnetic assembly of particles. The $M(H)$ curves measured at $T = 120$, 160 and 220 K were fitted simultaneously with a Langevin function weighted by a lognormal distribution (Fig. 5). An average magnetic moment $\mu_{120K} = 64\ (2)\ \mu_B$ per particle and a mean monodomain size of 7.3 nm with $\sigma = 0.33$ were obtained. Notice that for increasing temperature the inverse of the susceptibility departs from the linear SPM behaviour (see inset Fig. 3), signaling an increase of the PM thermal fluctuation of the surface spins. As a consequence the magnetic moment

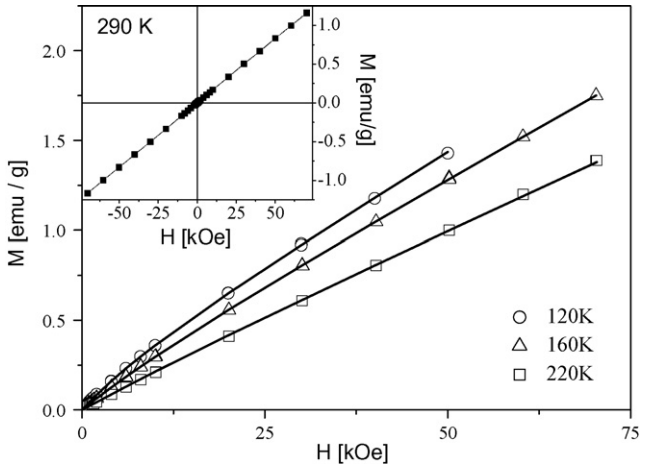

Fig. 5. $M(H)$ dependence measured at different temperatures $T_B < T < T_N$. Inset: $M(H)$ curve measured at $T = 290\,K > T_N$.

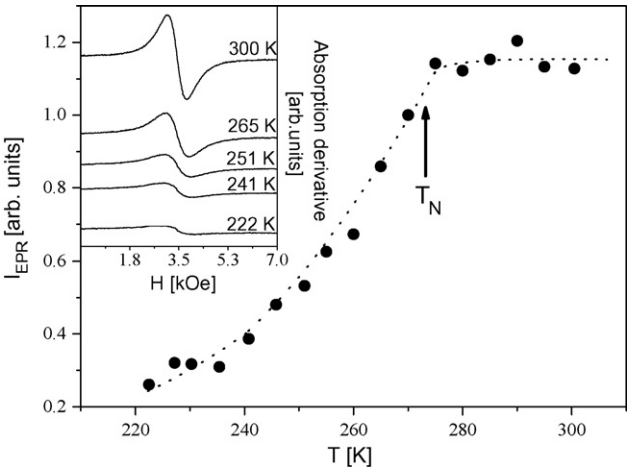

Fig. 6. EPR intensity as a function of temperature. Inset: EPR spectra recorded at different temperatures.

per particle diminishes for $T > 210\,K$. For example we have obtained $\mu_{160\,K} = 53\,(2)\,\mu_B$ and $\mu_{220\,K} = 38\,(2)\,\mu_B$.

Below the blocking temperature the ZFC–$M(H)$ presents two contributions: a saturating contribution due to the non-compensated magnetic moment of the ordered core and a component that does not saturate up to 7 T. In Fig. 4 the temperature dependence of the coercive field (Hc) is reported. From this figure it can be observed that the system does not follow the dependence $Hc \propto T^{1/2}$ as it is predicted for a system of identical non-interacting particles [7].

Although the system presents a narrow size distribution, the nanoparticles magnetic behaviour cannot be interpreted with current models that usually do not include the presence of interactions. Taking into account the magnetic moment of a nanoparticle $\langle\mu\rangle \sim 64\,\mu_B$ and the average distance between them we can estimate the dipolar field that interact with a particle which is smaller than 10 Oe. Therefore we cannot attribute to the dipolar field the interaction effect that we are observing. In previous studies exchange bias field has been measured in several AFM nanoparticle as Cr_2O_3 [8], α-Fe_2O_3 [9], NiO [10], so the effect of the intraparticle interactions could be more important than the interaction between the particles. In order to gain a more complete understanding about the intraparticle interaction we performed FC–$M(H)$ measurements. The samples were cooled from 300 K to different temperatures $T < T_B$ with an applied field of 50 kOe. The obtained loops present a shift towards negative field that rapidly decreases as the measuring temperature approaches T_B, but no coercive field enhancement was observed. This exchange bias field (H_{ex}), showed in Fig. 4, is an indication of the presence of an exchange interaction between the disordered surface magnetic structure and a core with antiferromagnetically ordered structure.

The EPR experiment is a more sensitive technique to magnetic transitions; therefore it allowed us to gain insight into the magnetic ordering of the Cr_2O_3 nanoparticles. In AFM system below the order temperature, large anisotropy and exchange fields are present so the resonance mode could not be excited, therefore T_N can usually be well determined when the EPR spectra disappears. In the inset of Fig. 6 we present the EPR spectra measured at different temperatures. These spectra consist of a single absorption line centred at $g = 1.96 \pm 0.01$, that corresponds to the PM resonance of the Cr^{3+} ions. In Fig. 6 we show the temperature dependence of the EPR intensity (I_{EPR}), calculated as $\Delta H_{pp}^2 \times h_{pp}$, where ΔH_{pp} is the peak-to-peak line width and h_{pp} is the peak-to-peak amplitude. From this figure a remarkable decrease of the signal can be observed at $\sim$270 K. This behaviour confirms that T_N shifted to lower temperature compared with the bulk value (T_N(Bulk) $\sim$ 308 K), in agreement with the PM behaviour observed in the magnetization measurements at room temperature. On the other hand, we still observed a PM signal below T_N, which it is attributed to a disorder surface.

The results obtained by EPR experiments complement the magnetization measurements and support the core–shell nanoparticle model. In this system the core magnetic order temperature is reduced as a consequence of the size effects, the uncompensated magnetic moment shows superparamagnetic behaviour and interacts with the surface spins showing exchange bias properties. This picture contrasts with previous results that we have obtained in Cr_2O_3 nanoparticles of larger size $30\,nm \leq \phi \leq 70\,nm$ [11]. In Ref. [11] we reported the magnetic anisotropy as a function of the nanoparticle size. In the studied range the nanoparticles do not show superparamagnetic behaviour, however, for smaller diameter at low temperature the energy barrier will be comparable to the thermal energy so the superparamagnetic regime could be reached in agreement with the experimental observation. Besides, we have observed that for larger nanoparticles size the uncompensated magnetic moment is almost negligible and does not present exchange bias properties.

4. Conclusions

In summary, we report the magnetic properties of AFM Cr_2O_3 nanoparticles with narrow size distribution centred at 7.8 nm. We observed that the AFM order temperature is reduced to $T_N = 270\,K$ with respect to the bulk value ($T_N = 308\,K$). Below T_N the nanoparticles present a magnetic moment that shows superparamagnetic behaviour. From the fit of the $M(H)$ curves we obtained a magnetic moment per particle of $\sim 64\,\mu_B$ and a mean monodomain size of 7.3 nm. At $T_B = 28\,K$ the system present a change from superparamagnetic to blocked regime, and the sample evidence the effect of interactions. We observed exchange bias field of $\sim$400 Oe at low temperature which implies the existence of exchange interaction between the surface spins and the spins at the core.

Acknowledgements

This work has been accomplished with partial support of ANPCyT, Argentina through Grant No. PICTs 3–13294, 4–25317 and 20770; Conicet, Argentina through Grant No. PIP 5250/03; and U.N. Cuyo through Grant No. 06/C275.

References

[1] L. Néel, Compt. Rend. 252 (1961) 4075.
[2] J.T. Richardson, D.I. Yiagas, B. Turk, K. Foster, J. Appl. Phys. 70 (1991) 6977–6982.
[3] S. Mørup, D.E. Madsen, C. Frandsen, C.R.H. Bahl, M.F. Hansen, J. Phys.: Condens. Matter 19 (2007) 213202.
[4] C.G. Shull, W.A. Strauser, E.O. Wollan, Phys. Rev. 83 (1951) 333.
[5] M. Bañobre-López, C. Vázquez-Vázquez, J. Rivas, M.A. López-Quintela, Nanotechnology 14 (2003) 318–322.
[6] J.L. Dormann, D. Fiorani, M. El Yamani, Phys. Lett. A 120 (1987) 95–99.
[7] J.L. Dormann, D. Fiorani, E. Tronc, Adv. Chem. Phys. 98 (1997) 283–494.
[8] S.A. Makhlouf, J. Magn. Magn. Mater. 272–276 (2004) 1530–1532.
[9] R.D. Zysler, M. Vasquez Mansilla, D. Fiorani, Eur. Phys. J B41 (2004) 171–175.
[10] S.A. Makhlouf, F.T. Parker, F.E. Spada, A.E. Berkowitz, J. Appl. Phys. 81 (1997) 5561–5563.
[11] D. Tobia, E. Winkler, R.D. Zysler, M. Granada, H. Troiani, Phys. Rev. B 78 (2008) 104412.